Basic Experiments on Measurement of Salinity using a Heterodyne Double-pass Interferometer

Kenichi Asakawa and Yasuhisa Ishihara
Marine Technology and Engineering Center
Japan Agency for Marine–Earth Science and Technology
Yokosuka-shi, Kanagawa, Japan

Akito Araya
Earthquake Research Institute
The University of Tokyo
Bunkyo-ku, Tokyo, Japan

***Abstract*—We propose a new method to measure the salinity of seawater using a heterodyne double-pass interferometer. Results of preliminary experiments show that the effect of the temperature was reduced by about one order of magnitude when compared with Michelson interferometer. The measured phase difference between pure water and 3.5 ‰ salt water of 182.0 degrees was slightly higher than that of the theoretically expected value of 176.0 degrees. The possible cause of this error is discussed in this paper.**

Keywords—salinity; heterodyne double-pass interferometer; Zeeman effect; HeNe laser; ocean environment; salinity

I. INTRODUCTION

Seawater serves an important role in climate stabilization because it has 1,000 times higher thermal capacity than the atmosphere. According to the Inter-Governmental Panel on Climate Change (IPCC), seawater stores more than 90% of Earth's artificially generated heat. Even a small change in seawater conditions would greatly influence our long-term climate. To predict climate change precisely, it is important to elucidate the relation of seawater to climate.

Seawater salinity is closely related with its density, which controls seawater and heat circulation. For that reason, seawater salinity, temperature, and pressure are monitored at many points from the sea surface to deep waters.

Salinity is commonly measured by monitoring seawater conductivity. Although typical conductivity sensors have sufficient resolution of about 1×10^{-5} Ωm, its long-term stability is inadequate. Therefore, these sensors should be calibrated annually, which increases operation costs.

On the other hand, the refractive index of seawater is well known to have a clear relation with number of molecules, as shown in (1). We can use this relation to estimate seawater density.

$$\frac{n^2-1}{n^2+1} = \frac{4\pi}{3} N\alpha \qquad (1)$$

In that equation, n, N, and α respectively denote the refractive index, the number of molecules in a certain volume, and polarization of molecules.

This work was supported by JSPS KAKENHI Grant Number 25610143.

To date, several studies relevant to measuring the refractive index of seawater have been reported. Mahrt and Kroebel showed that the difference of refractive index of reference and measuring liquid can be measured using a Michelson interferometer with an accuracy of 0.005 psu [1], [2]. They exchanged reference and measuring liquid in cells of 40 mm long, and then counted fringes.

Mahrt and Waldmann [3] developed a refractometer in 1998 that enables high-speed profiling. Their refractometer reportedly had high precision of 10^{-6}. Later, Mahrt and Hosseinioun [4] developed an expendable refractometer with maximum operating depth of 6,000 m.

Alford et al. [5] proposed another optical method to measure the refractive index. They used fused optical fibers, and showed it can provide accuracy of better than 10^{-8} and spatial resolution of 1 mm. Those are sufficient accuracy and resolution, but they have not demonstrated long-term stability.

The ultimate goal of this study is to develop a small optical salinometer with high accuracy and long-term stability. In an earlier paper [6], we proposed a new optical method using a heterodyne Michelson interferometer to measure the refractive index. We made a compact Michelson interferometer and measured the difference of refractive indexes between pure water and 3 ‰ salt water. The averaged phase difference of 154° coincides with the theoretically expected value of 156° within an accuracy of $\pm 1.6 \times 10^{-5}$. We confirmed that the measurement error is mainly caused by deformation of the corner reflectors because of temperature change.

To reduce the measurement error described above, we introduced a heterodyne double-pass interferometer [7] and conducted preliminary tests. As described herein, we present an outline of the heterodyne double-pass interferometer and the results of the preliminary tests.

II. CONFIGURATION OF THE HETERODYNE DOUBLE-PASS INTERFEROMETER

Fig. 1 portrays the basic configuration of the heterodyne double-pass interferometer. We use a frequency-stabilized 633 nm axial Zeeman HeNe laser as a light source (NOE-9111; Neoark Corp.). This laser simultaneously emits two circularly polarized lights. The oscillation frequency difference between them is about 1 MHz.

978-0-933957-43-5 ©2015 MTS

This is a DRAFT. As such it may not be cited in other works.
The citable Proceedings of the Conference will be published in
IEEE Xplore shortly after the conclusion of the conference.

These two circularly polarized beams are converted by a 1/4 wavelength plate to two mutually perpendicular linearly polarized lights. This 1/4 wavelength plate is mounted in the housing of the laser. It is not presented in Fig. 1. The beams are then transmitted to the interferometer. The blue and red dotted lines respectively portray two linearly polarized lights with oscillation frequencies of f1 and f2. Hereinafter, we respectively designate these lights as the blue beam and red beam. As described above, the difference between f1 and f2 is about 1 MHz. Black lines in Fig. 1 show that both beams are overlapped and that they propagate on the same path.

A part of two beams are taken out by a non-polarizing beam sampler at the input stage. The reflection coefficient of the beam sampler is about 5%. The beat-signal of the separated beams is detected using a polarizer and an optical detector. The detected beat signal is used as a reference signal.

Then the two beams enter into the polarizing beam splitter. At this point, the blue beam is transmitted through the polarizing beam splitter. The red beam is reflected by the polarizing beam splitter. The beams, after reflection by corner reflectors, return to the polarizing beam splitter. 1/4 λ plates are inserted in the optical path. When beams are passing through the 1/4 λ plates two times, the polarization angles rotate by 90 deg. Therefore when these beams return to the polarizing beam splitter, the blue beam is then reflected and the red beam is transmitted by the polarizing beam splitter. These two beams then mutually overlap and enter into the third arm of the interferometer.

Two beams, after reflection by three corner reflectors, pass through three arms of the interferometer. A cell in which salt water is filled is placed in one of the arms. Only the blue beam passes through the cell. Both beams pass through almost identical paths except the cell portion. Consequently, even if deformation of the interferometer occurs because of temperature change for example, its effect is almost cancelled.

Two beams finally overlap again. Their beat signal is detected using another polarizer and optical detector. The detected interference signal is sent to the lock-in amplifier (Signal Recovery 7280; Advanced Measurement Technology Inc.). The phase difference between the reference signal and the detected signal is measured and recorded.

We measure the difference of the refractive index between the pure water and the salt water by filling the cell alternately with the pure water and the salt water. The phase difference when the cell is filled with the pure water and with salt water is

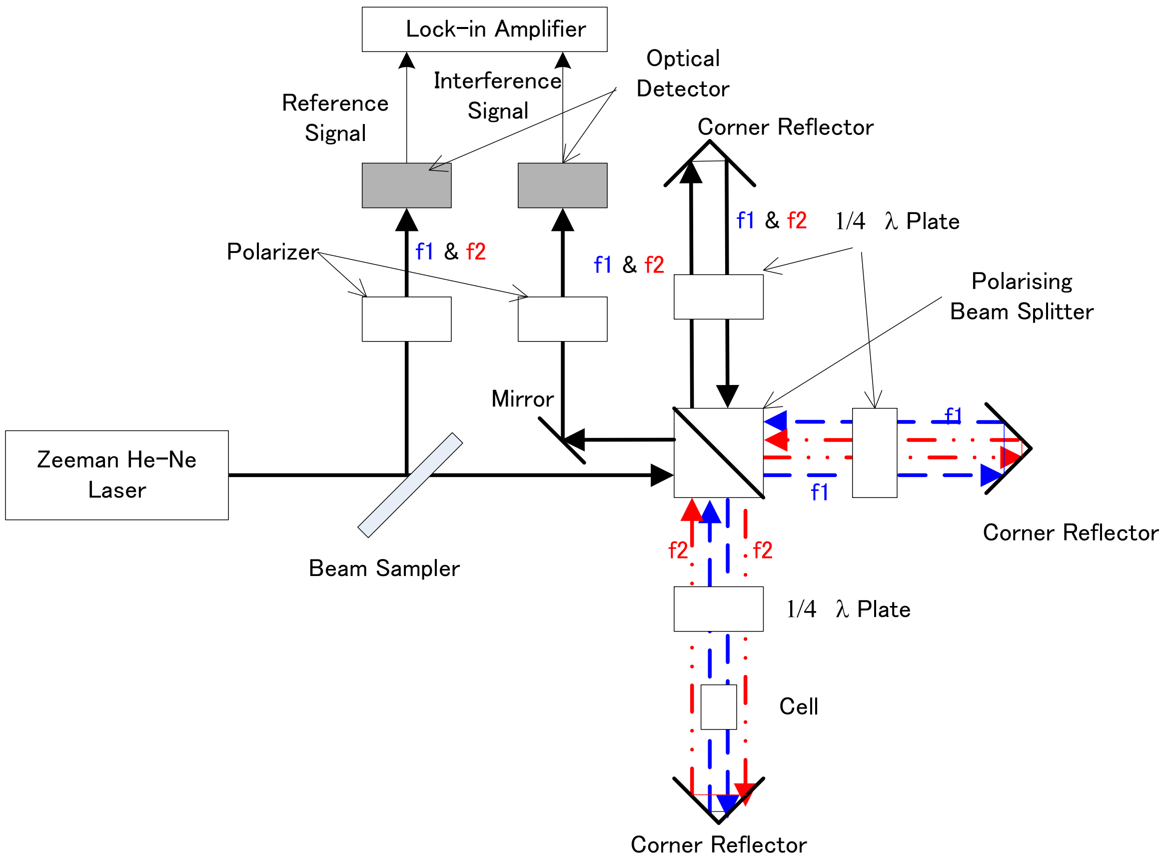

Fig. 1 Configuration of the heterodyne double-pass interferometer:
f1 and f2 denote oscillation frequencies.

presented as the following equation.

$$\Delta\theta = 4\pi L / \lambda \Delta n$$

Therein, Δn, L and λ respectively denote the difference of the refractive index between the pure water and the salt water to be measured, the cell thickness, and the wavelength.

Fig. 2 presents the relation between salinity and the refractive index [8]. These data are for the sodium D line (λ= 589 nm). Therefore, when a He–Ne laser is used as a light source, a slight modification is necessary. However, because this modification is small, we use this relation directly in this study.

III. Experimental Setup

Fig. 3 presents a photograph of the experimental setup. The interferometer was built using a set of optical components on a vibration isolation system. The interferometer was covered with an acrylic box to stabilize the temperature variation.

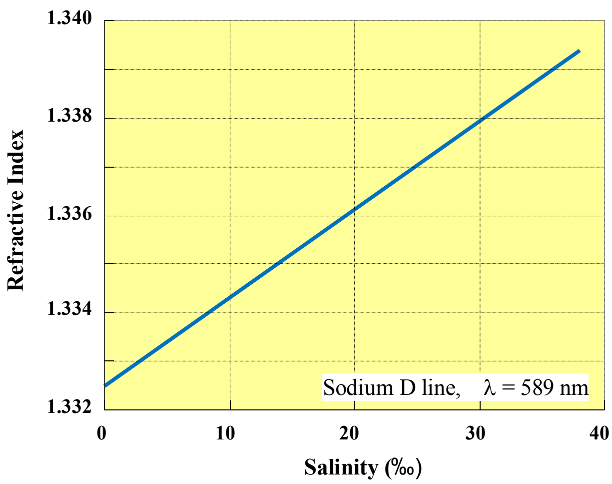

Fig. 2 Relation between salinity and refractive index.

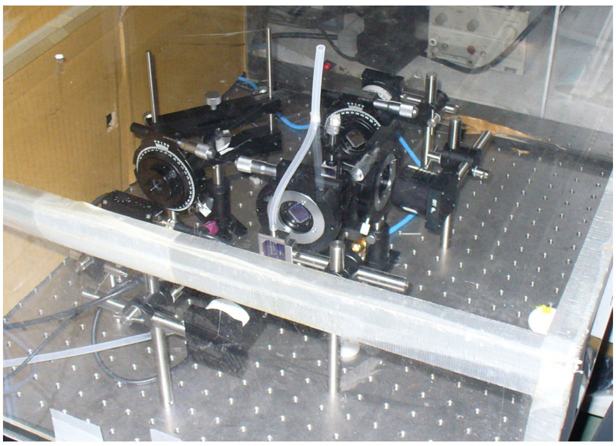
Fig. 3 Photograph of the experimental setup.

A 0.25-mm-thick cell (Fig. 4) was used. Salt water and pure water were filled into the cell alternately through flexible tubes. The cell surfaces were coated for antireflection. The water, filled through the upper inlet, is drawn through the lower outlet. The width of the portion where saline and pure water were filled is 6 mm. The blue beams in Fig. 1 pass through the portion filled the water; the red beams pass through the outside of that portion.

Fig. 5 portrays the waveform of the reference signal and the interference signal recorded using a digital oscilloscope. The beat frequency was about 1 MHz; the visibility of the interference signal was about 0.69.

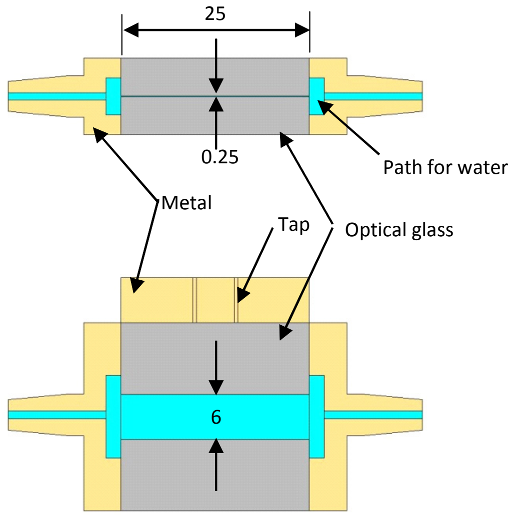

Fig. 4 Cross section view of the cell.
unit: mm

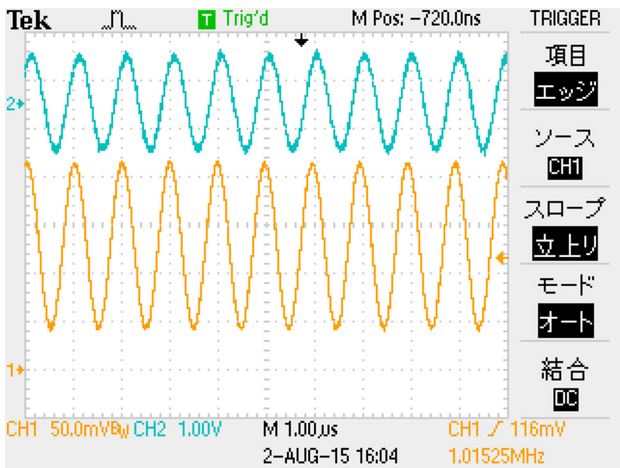

Fig. 5 Waveform of the beat signal.
Upper: blue line shows the reference signal. Lower: orange line shows the interference signal

IV. Experimental Results

Before measuring the difference between the refractive indexes between salt water and pure water, we monitored the phase variation of the interferometer without a cell for 56 hr to evaluate the stability of the heterodyne double-pass interferometer. During the test, although the temperature variation of about 2 °C was recorded, fluctuation of the phase difference was within 8 deg, as depicted in Fig. 6. In the case of a Michelson interferometer, phase variation of about 80 deg was recorded against temperature variation of 1 °C, as portrayed in Fig. 7 [6]. By introducing the heterodyne double-pass interferometer, the phase difference variation was lowered by about one order of magnitude. The clear correlation between temperature variation and the phase fluctuation has been lowered as depicted in Fig. 6. We think the effects of ambient temperature change have been almost removed.

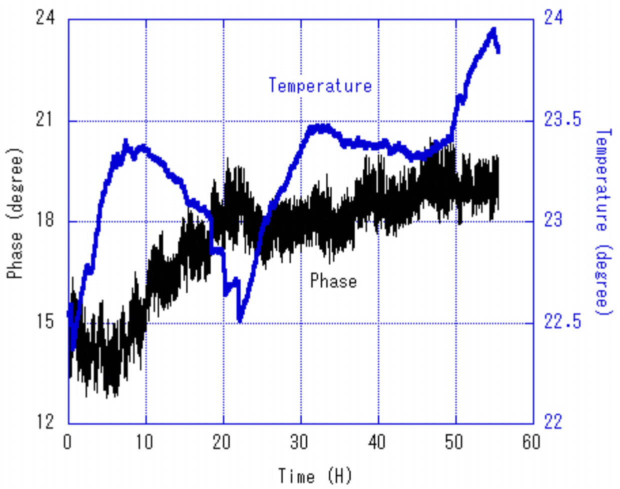

Fig. 6 Fluctuation of the phase difference of the heterodyne double-pass interferometer and temperature variation.

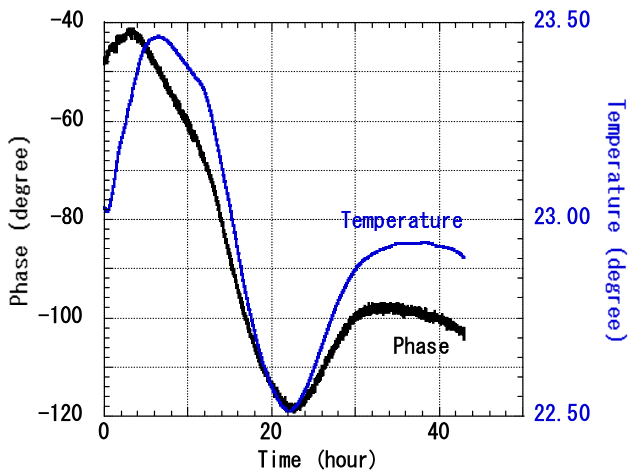

Fig. 7 Example of measured phase variation and temperature at the interferometer.

Then, differences of refractive indexes between the pure water and salt water were measured. Fig. 8 portrays an example of the recorded phase change where the pure water and the 3.5 ‰ salty water were alternately inserted into the cell using syringes. To exchange the water in the cell thoroughly, we evacuated the cell before re-filling the cell. Phase differences were averaged for about four minutes. Then the difference between adjacent averaged data was calculated. The average and the standard deviation of the phase differences were, respectively, 182.0 and 3.0. Assuming that the relation between the salinity and the refractive index against sodium D line (589 nm) is applicable to HeNe laser (633 nm), the expected phase shift is expected to be 176.0 deg, which is slightly lower than the experimentally obtained results. Furthermore, we can find variation and gradual shift of the measured phase in Fig. 8. We conducted the same measurements on another day and obtained similar results.

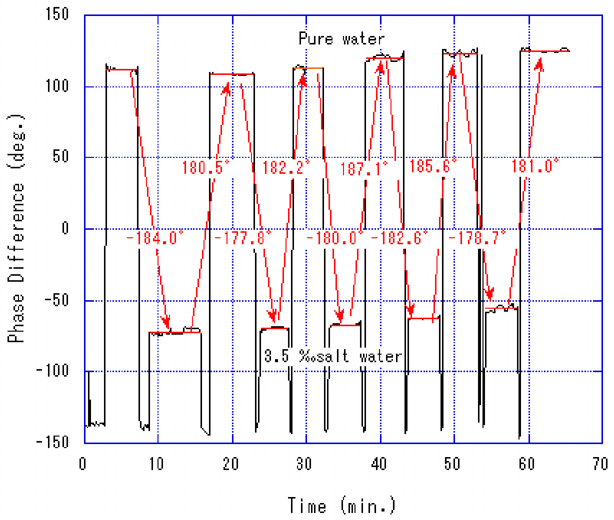

Fig. 8 Example of measured phase difference variation while alternately filling the cell with pure water and 3.5 ‰ salt water.

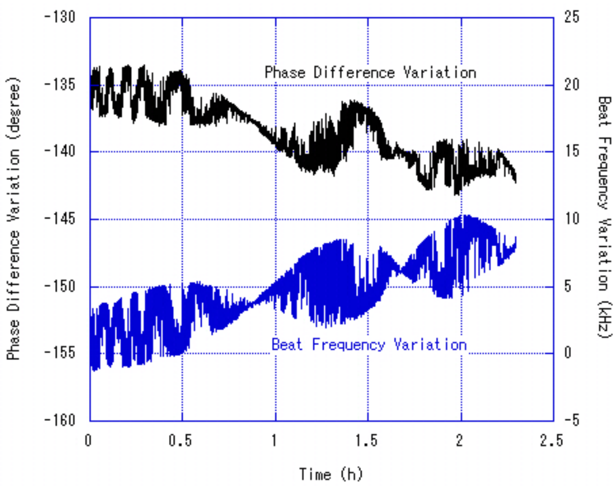

Fig. 9 Correlation between the phase difference variation and beat frequency variation.

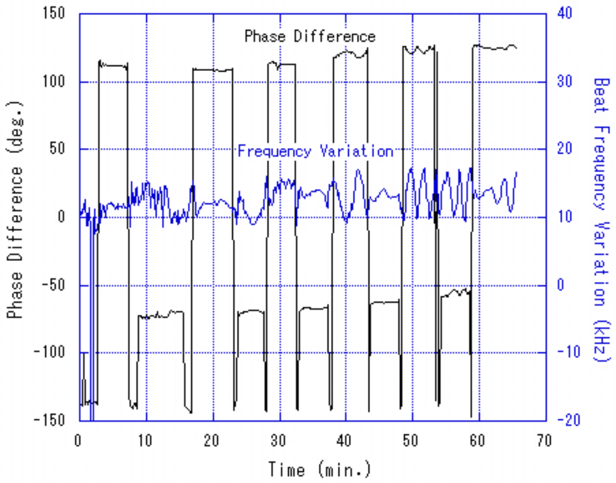

Fig. 10 Phase difference variation and beat frequency variation while alternately filling the cell with pure water and 3.5 ‰ salt water.

To ascertain the cause of this variation and gradual shift in the measured phase difference, we compared the phase difference and the beat frequency variation. The beat frequency variation was also measured using the same digital lock-in amplifier. Figure 9 presents an example of experimentally obtained results. In this measurement, the cell is removed. Only the phase variation and the beat frequency variation were measured. Although the magnitude of the beat signal fluctuation was several kilohertz, i.e., two or three orders of magnitude smaller than the beat signal's frequency of 1 MHz, a clear relation is apparent between the beat frequency variation and the phase difference variation. In Fig. 10, the beat frequency variation is added to the data presented in Fig. 8. We can also find a clear relation between them. The beat frequency variation clearly affected the phase difference. The beat frequency is proportional to the magnitude of the magnetic field applied to the HeNe gas tube. Therefore, we can control and stabilize the beat frequency and lessen its effect on phase difference variation. We are now analyzing how the beat signal variation affects the phase difference of the interferometer.

Possible causes of error also include error of cell thickness, error of the sample salinity, difference of refractive indexes for sodium D line and HeNe laser, mixing of pure water and salt water, temperature differences between the cell and the sample water, and mixing of blue and red beams attributable to imperfections of polarizing beam splitters and polarizers. We plan to analyze these error sources and their effects on measurements.

V. CONCLUSION

We have proposed the use of a heterodyne double-pass interferometer to measure salinity. Assessment of the effects of ambient temperature variation on measurements confirmed that its effects were reduced by about one order of magnitude from those of a heterodyne Michelson interferometer. The effects of ambient temperature change have been almost removed.

The phase difference between 3.5 ‰ salt water and pure water was measured to evaluate the proposed method. Results show that the measured phase difference of 182.0 deg was slightly larger than the theoretically estimated value of 176.0 deg. As a main source of the error, we have pointed out the effects of the variation of the beat frequency of the frequency-stabilized 633 nm Zeeman HeNe laser. Results show a close relation between them. The beat frequency is proportional to the magnitude of magnetic field applied to the HeNe gas tube. Therefore, we can control and stabilize the beat frequency fluctuation and reduce its effects on the phase difference. We are now analyzing how the beat signal variation affects the phase of the interferometer. We have also pointed out some possible error sources. Future studies will analyze these error sources and their effects on measurements.

REFERENCES

[1] K.-H. Mahrt and W. Kroebel, "Optical Interferometric Bench Salinometer of high precision with electronical read out," *Proc. OCENAS'84*, pp. 219-223, 1984.

[2] K.-H. Mahrt and W. Kroebel, "Quantitative performance data of a new automatic optical bench salinometer/densitometer," *Proc. of OCEANS'85*, pp. 622-627, 1985.

[3] K.-H. Mahrt and C. Maldmann, "Field proven high speed micro optical density profiling sampling 1000 teimes per second with 10-6 precision," *Proc. of OCEANS'88*, pp. 497-504, 1988.

[4] K.-H. Mahrt and A. Hosseinnioun, "Expendable optical density profilers started from intelligent multiple shot launcher on the deep sea bottom with storage capabilities over several years," *Proc. of OCENS 2000*, pp. 791-796, 2000.

[5] M. H. Alford, D. W. Gerdt, and C. M. Adkins, "An ocean refractometer: Resolving millimeter-scale turbulent density fluctuations via the refractive index," *J. of Atomos. and Ocean. Techn.,* vol. 23, pp. 121-137, 2006.

[6] K. Asakawa, Y. Ishihara, Y. Takahashi, T. Sugiyama, and A. Araya, "Basic experiments on measurement of salinity using a heterodyne Michelson interferometer," Oceans 2010 MTS/IEEE Seattle, 2010.

[7] K. Fujii, E. R. Williams and R. L. Steiner and D. B. Newell, "A new refractometer by combining a variable length vacuum cell and a double - pass Michelson interferometer," *IEEE Trans. Instrum. Meas*., vol. 46, pp. 191-195, 1997.

[8] Handbook of Marine Engineering (in Japanese), edited by JOGMEC.